Conf-940391--3

UCRL-JC-115105
PREPRINT

Simulation and Analysis of Laser Guide Star Adaptive Optics Systems for the Eight to Ten Meter Class Telescopes

D. T. Gavel
S. S. Olivier
Lawrence Livermore National Laboratory

This paper was prepared for submittal to
SPIE's 1994 Symposium on Astronomical Telescopes &
Instrumentation for the 21st Century
Kona, Hawaii
13–18 March 1994

March 1994

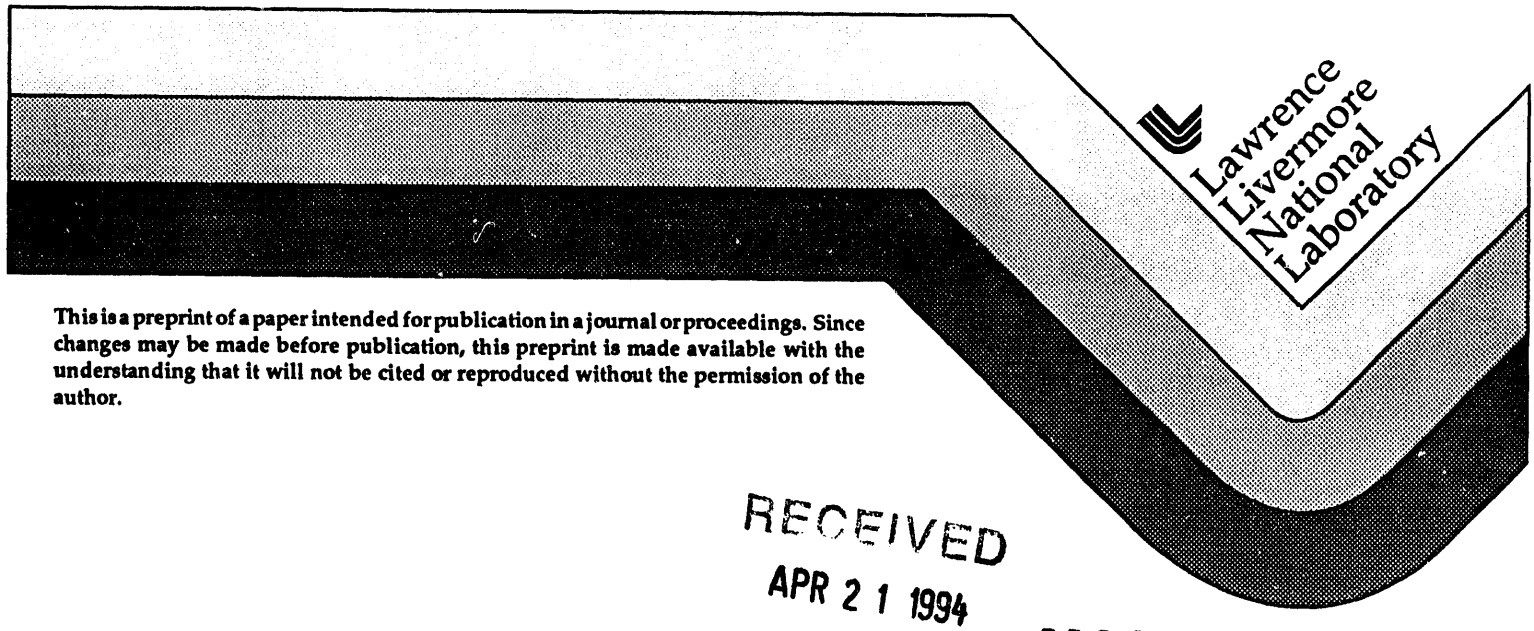

DISCLAIMER

Simulation and Analysis of Laser Guide Star Adaptive Optics Systems for the Eight to Ten Meter Class Telescopes *

D. T. Gavel and S. S. Olivier
Lawrence Livermore National Laboratory
Livermore, California

ABSTRACT

This paper discusses the design and analysis of laser-guided adaptive optic systems for the large, 8-10 meter class telescopes. We describe a technique for calculating the expected modulation transfer function and the point spread function for a closed loop adaptive optics system, parameterized by the degree of correction and the seeing conditions. The results agree closely with simulations and experimental data, and validate well known scaling law models even at low order correction. Scaling law model analysis of a proposed adaptive optics system at the Keck telescope leads to the conclusion that a single laser guide star beacon will be adequate for diffraction limited imaging at wavelengths between 1 and 3 μm with reasonable coverage of the sky. Cone anisoplanatism will dominate wavefront correction error at the visible wavelengths unless multiple laser guide stars are used.

1. INTRODUCTION

Adaptive optic systems have shown great promise for improving astronomical seeing beyond the resolution limits imposed by atmospheric turbulence.[1] Although efficient collectors of light, the larger aperture telescopes are not able to resolve objects any better than those with an aperture of approximately r_0, the characteristic size of wavefront phase variations. For excellent sites under the best seeing conditions, r_0 is about 20 cm, therefore, the best telescopes in the world resolve no better than a good amateur astronomer's 8-inch telescope.

With adaptive optics, the new class of 8 to 10 meter diameter telescopes, the existing Keck-I, the Keck-II and Subaru under construction, and the planned northern and southern hemisphere Gemini telescopes and planned Large Binocular Telescope, have the potential of becoming the highest resolution astronomical instruments, exceeding the Hubble space telescope by a factor of four. In the design of adaptive optics systems, the intended science goals must be kept in mind. For example, extrasolar planetary study benefits from high Strehl over a narrow field of view, whereas multiobject spectroscopy will benefit from a large corrected field with uniformly improved encircled energy radius. The factors that enter into consideration in the design of an adaptive optics system include the intended observation wavelengths, the shape of the optical point spread function, the variation in point spread over the field of view, the fraction of the sky available for correction by the system at a given wavelength, and the expected percentage of observing time when adaptive optics correction goals can be met given the variation in seeing conditions at the site. These considerations determine the number of deformable mirror degrees of freedom required, the wavefront reconstruction algorithm to be used and, the choice of wavefront sensor.[2]

To achieve reasonable sky coverage for wavelengths shorter than 3 microns, a *laser guide star* must be used. This is because in these bands the wavefront phase decorrelation time is so short (a few tens of milliseconds in the visible) that a 10'th magnitude or brighter reference star must be used. The phase also decorrelates over a small angle called the isoplanatic angle, which is only a few arcseconds in the visible. The chances of finding a 10'th magnitude star that close to an arbitrary point on the sky are very slim. There has been considerable work in the area of low order correction, which, presumably can take advantage of the larger isoplanatic angles and longer decorrelation times of the low order Zernike modes, resulting in partial correction at a larger separation angle, however, it turns out that except for a few of the very lowest

* Work performed under the auspices of the U. S. Department of Energy by the Lawrence Livermore National Laboratory under contract number W-7405-eng-48

order modes (tip, tilt, focus, astigmatism) the isoplanatic angle associated with the modes is roughly the isoplanatic angle of the overall wavefront.[3] Certainly beyond 2 microns, in most expected seeing conditions, the isoplanatic angle becomes so small that natural guide star based systems are limited to imaging only near bright objects (extrasolar planetary studies falls into this class of observations).

The laser is attached to the telescope and therefore the guide star is steerable to any point on the sky. This solves the main problem of anisoplanatism, but introduces another milder anisoplanatism due to the finite altitude and finite size of the projected artificial guide star.[4] A sodium layer guide star is formed much higher (90 km) than a guide star based on Rayleigh backscatter. The higher altitude star minimizes the cone angle anisoplanatism, and allows the adaptive optics on the larger telescopes to operate in the 1–3 μm range with only a single guide star. But even with the high altitude sodium guide star, cone effect will be dominant in the 0.5–1 μm range, and multiple guide stars may be necessary. We consider only sodium guide stars in the analysis given in this paper. When using a laser, the background noise due to scatter of laser light from the lower atmosphere must be rejected. Since the laser light is narrow band, a notch rejection filter can be used to keep the laser light out of the science camera. To keep the light out of the wavefront sensor, the laser is projected either offset from the side of the telescope or from behind the secondary. The occlusion prevents direct scatter into the telescope, and a field stop at the guide star focus rejects the lower altitude light, since this light is off axis and focuses behind the guide star focus.

A key consideration in the design is the order of adaptive optic correction, that is, the number of degrees of freedom available to the deformable mirror and wavefront reconstructor. The large telescopes will have $D/r_0 \approx 50$ in the mid-visible wavelengths, which implies thousands of degrees of freedom if diffraction-limited performance is desired. The point spread function of the corrected system does not degrade gracefully with respect to degrees of freedom either. Instead, there is an abrupt change when the corrected wavefront is phased (that is, within $\lambda/2$ over most of the aperture) at which point a diffraction limited core starts to appear on top of the seeing disk size halo. The lower order corrections, while not forming a core, do give slightly better than the seeing disk, as the analysis described in Section 2 shows. There is a smooth change in the point spread function as correction order is increased gradually shrinking the atmospheric seeing disk radius as energy is taken out of the far edge and packed toward the middle. The point of phasing occurs when the corrected disk diameter (defined as the angle at which the intensity is half the maximum) reaches about one half the original seeing disk diameter. Then, as correction is further increased, more energy is taken out of the halo and put into the core.

There is a critical number of degrees of freedom needed to achieve a diffraction-limited core, roughly one for each correlation area (r_0) on the telescope aperture. This is true regardless of whether a modal or zonal reconstruction algorithm is used. The analysis by Noll[5] describes the correction error due to optimally fitting a Kolmogorov statistical wavefront to a truncated Zernike series. If each Zernike mode is considered a modal degree of freedom, then n modal degrees of freedom give roughly the same fitting error as n modal degrees of freedom. The error in both cases scales with $(D/r_0)^{5/3}$ and differ only slightly in the coefficient, which depends on the nature and quality of the deformable mirror. In practice, Zernike modes are hard to produce cleanly with deformable mirrors, so there is an additional fitting error associated with each of the corrected modes.

In Section 2 we describe the methods used in analysis and prediction of adaptive optics systems performance. These prediction methods have been borne out be experiments performed by the Lawrence Livermore group at the Lick observatory 40 inch telescope.[6] Section 3 presents performance predictions for an adaptive optics system mounted on the Keck telescope. The results are relevant to any of the 8-10 meter class telescopes. We conclude with a discussion of the issues and problems that need to be further addressed for visible wavelength and wide field imaging.

2. MODELING DESCRIPTION

The adaptive optic system performance can be described most succinctly in terms of the system Strehl ratio, that is, the (ensemble average) peak magnitude of the point spread function relative to the diffraction limited point spread function. System performance analysis, optimization, and design can be guided by estimating the Strehl under various observing wavelengths, seeing conditions, field angles (separation from guide star), guide star magnitude, etc. Simple scaling laws have been developed to calculate Strehl given system parameters such as deformable mirror interactuator spacing, laser power, and system bandwidth.

Reference 2 gives a review of these scaling laws and their use in optimizing design choices.

The expected Strehl is approximated by applying the well known Maréchal expression.[7]

$$S \approx \exp\left[-\sigma_{wf}^2\right] \tag{1}$$

where σ_{wf}^2 is the mean square wavefront variation from a flat reference. For an adaptive optics system the overall wavefront error is calculated by summing the squares of each system error contributor:

$$\sigma_{wf}^2 = \sigma_{servo}^2 + \sigma_{dm}^2 + \sigma_{meas}^2 + \sigma_{aniso}^2 \tag{2}$$

where σ_{servo} is the contribution due to finite servo bandwidth, σ_{meas} is the contribution due to signal to noise in the detector, σ_{dm} is the deformable mirror fitting error due to a finite number of degrees of freedom, σ_{aniso} is the reference beacon error due to anisoplanatism. The terms are further described in reference 2.

The approximation (1) is considered valid under Maréchal's condition, $\sigma_{wf} < \pi/2$ radians, which is equivalent to the phasing condition mentioned in the introduction. According to the formulas derived by Fried[8] one can plot the ensemble average Strehl vs wavefront variance for the uncorrected (long exposure) and tilt removed (short exposure) cases under the assumption of Kolmogorov phase statistics. Figure 1 shows these cases and similar curves for higher order correction computed using the method to be described in Section 2 below. It can be seen that the Maréchal approximation is valid for $S \approx> 0.1$. With adaptive optics correction, the approximation is valid over a larger range. Higher order systems (systems with more than 25 degrees of freedom) closely follow the Maréchal approximation down to Strehls of about 0.01.

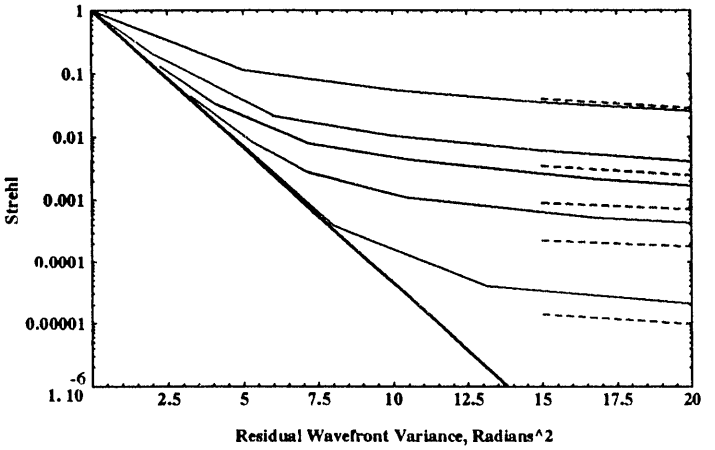

Figure 1 Strehl as a function of closed loop residual wavefront error, σ_{wf}^2. The Maréchal approximation $S = \exp[-\sigma_{wf}^2]$ is the bold solid line. Five cases are shown, from top to bottom: uncorrected, short exposure (perfect tip/tilt corrected), 20 DOF, 80 DOF, and 1500 DOF. DOF = degrees of freedom. (The last three cases are $D/\sigma = 5$, 10, and 43 respectively; σ is the influence width as defined in Section 2.) The dashed lines indicate the values of $(r_0/D)^2$ for each case, since $(r_0/D)^2$ is commonly used to approximate open loop Strehl.

The next level of performance modeling is to calculate the long exposure point spread function of the closed loop adaptive optical system. This has been worked out in principle by Welsh and Gardiner[9], but requires nested multiple integrals over regions that depend on the particular wavefront sensor and deformable mirror geometry. With some simplifying assumptions, that don't greatly affect the results, a general theory can be formulated. We follow the approach first used by Fried[8] in the case of long and short exposure images

and extend it to a general number of *zonal* degrees of freedom.

We start with a basic simplifying assumption: that the closed loop adaptive optic system acts as a spatio-temporal high-pass filter on wavefront fluctuations. The high pass nature takes into account the out of band fluctuations – wavefront spatial variations at frequencies greater than 1/2 the interactuator sampling period, and wavefront temporal variations faster than the closed loop servo response time. Considering first just the spatial filter, the model is

$$\tilde{\phi}(\mathbf{x}) = \phi(\mathbf{x}) - \int K(|\mathbf{x}-\mathbf{x}'|)\phi(\mathbf{x}')d\mathbf{x}' \tag{3}$$

where $\phi(\mathbf{x})$ is the uncorrected phase variation, and $\tilde{\phi}(\mathbf{x})$ is the residual phase variation remaining after correction. $K(x)$ represents a spatially invariant and circularly symmetric influence function which is associated with the combined effect of the Hartmann lenslet and deformable mirror actuator influence function. For ease in calculating transforms, we take this to be a Gaussian:

$$K(x;\sigma) \sim e^{(-x/\sigma)^2} \tag{4}$$

where σ is the influence width.

Define the structure functions $\mathcal{D}_\phi(r) = \langle[\phi(x+r) - \phi(x)]^2\rangle$ and $\mathcal{D}_{\tilde{\phi}}(r) = \langle[\tilde{\phi}(x+r) - \tilde{\phi}(x)]^2\rangle$, and the transform relationships[5]

$$\begin{aligned} \mathcal{D}_\phi(r) &= 2\int S_\phi(k)[1-\cos(2\pi\mathbf{k}\cdot\mathbf{r})]d\mathbf{k} \\ \mathcal{D}_{\tilde{\phi}}(r;\sigma) &= 2\int S_{\tilde{\phi}}(k;\sigma)[1-\cos(2\pi\mathbf{k}\cdot\mathbf{r})]d\mathbf{k}. \end{aligned} \tag{5}$$

$S_x(k)$ is the Weiner power spectrum of $\mathcal{D}_x(r)$ (x=ϕ or $\tilde{\phi}$). For Kolmogorov turbulence

$$\begin{aligned} \mathcal{D}_\phi(r) &= 6.88(r/r_0)^{5/3} \\ S_\phi(k) &= 0.023 r_0^{-5/3} k^{-11/3}. \end{aligned} \tag{6}$$

It is then straightforward to use (3) and (5) to derive the spectrum of the residual phase

$$S_{\tilde{\phi}}(k;\sigma) = [1 - K(k;\sigma)]^2 S_\phi(k) \tag{7}$$

where $K(k;\sigma) = \exp[-(\sigma k)^2]$ is the Fourier transform of $K(r;\sigma)$. Using (4), (6), (7) and then (5) we compute the structure function of the residual wavefront (the double integral in (5) is reduced to a single integral, the Fourier-Bessel transform, because of circular symmetry). We now invoke the argument surrounding equation (3.16) in reference 8 to calculate the ensemble average modulation transfer function (MTF) of the corrected system:

$$\langle\tau(f;\sigma)\rangle_{ao} = \tau_0(f)\exp[-\frac{1}{2}\mathcal{D}_{\tilde{\phi}}(\lambda R f;\sigma)] \tag{8}$$

where f is spatial frequency, and R is the focal length and $\tau_0(f)$ is the MTF of the unaberrated system

$$\tau_0(f) = (2/\pi)[\cos^{-1}(\lambda R f/D) - (\lambda R f/D)(1-(\lambda R f/D)^2)^{1/2}] \tag{9}$$

if $\lambda R f \leq D$ and 0 if $\lambda R f > D$.

In this derivation we have made three basic assumptions. First, that the spatial filtering due to adaptive optic correction is invariant with respect to shift, and ignores boundaries (such as the edge of the aperture). Second, we have ignored the discrete spatial sampling aspect (this effect is minor, since sampling in the spatial domain will alias the out of band spectrum from above the Nyquist frequency into the disturbance spectrum – but this spectrum falls off rapidly as $k^{-11/3}$). Third, we have used a near-field approximation in equation (8), ignoring the effects of scintillation. The major advantage is ease in computation: only one integral (5) needs to be calculated to compute a point in the MTF. The intensity point spread function (PSF) is then the Fourier-Bessel transform of the MTF.

The overall system is characterized by two parameters, D/σ and D/r_0, representing the degree of correction and the degree of atmospheric turbulence, respectively.

Figure 2 shows point spread functions for various values of σ/D illustrating the behavior at low order correction and the transition to formation of a core. For this graph, $D/r_0 = 16$ which is the case for the Keck telescope imaging near $\lambda = 1.25$ μm. Figure 3 shows corresponding encircled energy versus radius.

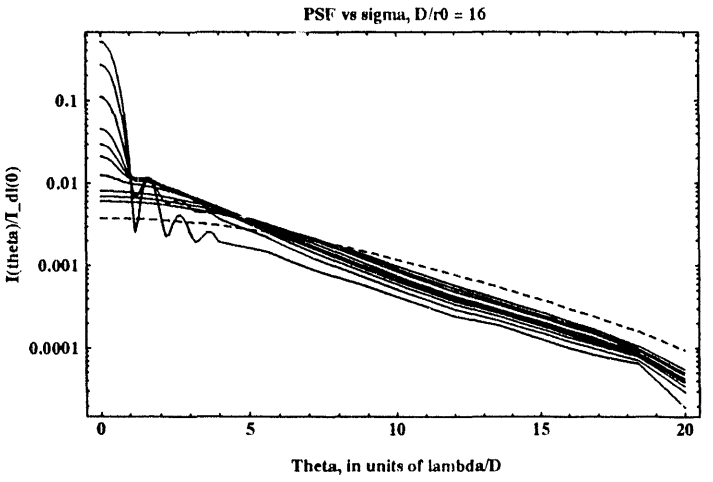

Figure 2 Point spread function for various degrees of freedom. $D/r_0 = 16$, which is the case for a 10 meter telescope in nominal seeing conditions on Mauna Kea observing at $\lambda = 1.25\mu$m. Curves are shown for $\sigma/D = 0.06$, 0.09, 0.125, 0.16, 0.18, 0.2, 0.25, 0.4, 0.6, 1.0 which corresponds to 218, 97, 50, 30, 24, 20, 12, 5, 2, and 1 degrees of freedom, respectively. Dashed line is the uncorrected seeing disk.

This analysis was used to plot points on the Strehl vs wavefront variance in Figure 1 using the facts that Strehl = PSF(0) and

$$\sigma^2_{wf} = \lim_{r\to\infty} -\frac{1}{2}\mathcal{D}_{\tilde{\phi}}(r;\sigma). \tag{10}$$

A similar line of reasoning, coupled with a frozen-flow hypothesis $\mathbf{x} = \mathbf{v}t$ gives the temporal power spectrum filter:

$$S_{\tilde{\phi}}(\omega,\theta) = [1 - K(\mathbf{k}\cdot\mathbf{v})][1 - K(\mathbf{k}\cdot\mathbf{v})]^* S_\phi(k) \tag{11}$$

where $\omega = \mathbf{k}\cdot\mathbf{v}$ is the temporal frequency, θ is the direction of the wind, and $\mathbf{v}$ is the wind velocity.

Typically, the closed loop servo system is represented by the high pass filter

$$K(\omega;\omega_c) = \frac{i\omega}{\omega_c + i\omega} \tag{12}$$

where ω_c is the control loop bandwidth.

A direction-independent power spectrum can be formulated by assuming that the wind is constant in magnitude and uniformly distributed in direction. Substituting (12) into (11) and averaging over wind direction θ, we get

$$S_{\tilde{\phi}}(k;\omega_c,v) = \frac{(kv)^2}{[(kv)^2+\omega_c^2]^{1/2}\{[(kv)^2+\omega_c^2]^{1/2}+\omega_c\}} S_\phi(k) \tag{13}$$

We now Fourier-Bessel transform the above power spectrum to generate the structure function $\mathcal{D}_{\tilde{\phi}}(\lambda Rf;\omega_c)$. The resulting modulation transfer function is then

$$\langle\tau(f;\sigma,\omega_c)\rangle_{ao} = \tau_0(f)\exp[-\frac{1}{2}\mathcal{D}_{\tilde{\phi}}(\lambda Rf;\sigma)]\exp[-\frac{1}{2}\mathcal{D}_{\tilde{\phi}}(\lambda Rf;\omega_c)] \tag{14}$$

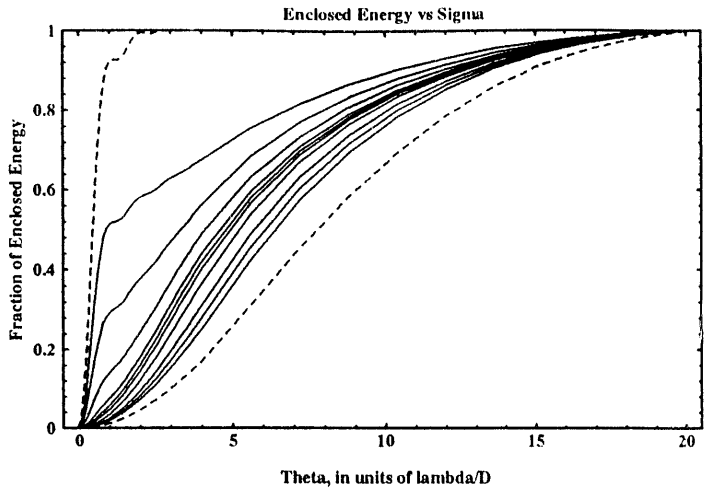

Figure 3 Enclosed energy for various degrees of freedom (corresponding to PSFs in Figure 2). $D/r_0 = 16$, which is the case for a 10 meter telescope in nominal seeing conditions on Mauna Kea observing at $\lambda = 1.25\mu$m. Curves are shown for $\sigma/D = 0.06$, 0.09, 0.125, 0.16, 0.18, 0.2, 0.25, 0.4, 0.6, 1.0 which corresponds to 218, 97, 50, 30, 24, 20, 12, 5, 2, and 1 degrees of freedom, respectively. Dashed lines show the diffraction limit and the uncorrected seeing disk.

which takes into account both spatial and temporal effects.

3. PERFORMANCE PREDICTIONS FOR 8–10 METER TELESCOPES

The point spread function and enclosed energy curves of Figures 2 and 3 predict the performance of adaptive optics systems on the Keck telescope at an imaging wavelength near 1.25 μm, assuming a single adequately bright laser guide star. Strehl performance predictions versus wavelength and laser power for the Keck telescope are shown in Figures 4 and 5 respectively. The scaling laws of reference 2 and equations (1) and (2) are used to generate these curves.

The Strehl dependence on laser power is illustrated in Figure 5. Current laser technology appropriate to generating sodium layer guide stars falls into two classes: CW and pulsed. The CW laser has the advantage of low average illumination (Watts/cm^2) at the sodium layer resulting in a nearly linear response of guide star signal to laser power. Unfortunately, present CW laser technology is limited to a few watts output power. While this may be suitable for adaptive optics in the infrared wavelengths, the laser power requirements scale rather rapidly with observing wavelength ($\sim \lambda^{-28/5}$).[2] Pulsed dye lasers have been demonstrated at kilowatt levels.[10]

Sky coverage for laser and natural guide star systems is shown in Figure 6. Sky coverage with the laser guide star system is limited by the isoplanatic angle of the tip/tilt reference[11] since the sodium guide star cannot itself be used as a tip/tilt reference. Long exposure Strehl is degraded by tilt errors according to

$$S_{le} = S\left[\frac{(\lambda/D)^2}{(\sigma_\alpha/0.82)^2 + (\lambda/D)^2}\right] \tag{14}$$

where S is the higher order Strehl (equation 1) and σ_α^2 is the variance of the tilt error. Strehl performance of the laser guide star system is degraded somewhat by anisoplanatism in the tilt reference, but not nearly

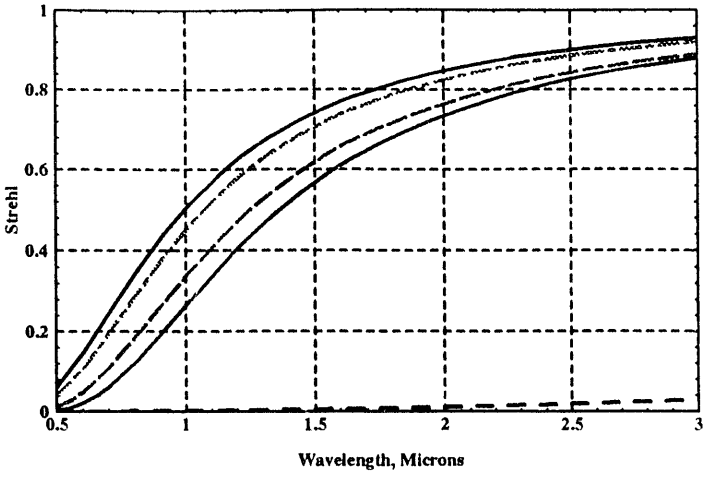

Figure 4 Strehl vs wavelength for a Keck 10 meter telescope adaptive optics system. 273 degrees of freedom in the deformable mirror is assumed and control bandwidth is optimized by trading servo lag error for signal photons in each case. Seeing conditions are $r_0 = 20$ cm, $f_g = 50$ Hz, $\theta_0 = 20$ μr at $\lambda = 0.5$ μm. Cases shown are (5 curves, top to bottom) 10'th magnitude natural guide star, 300 Watt pulsed dye laser (30 kHz, 150 ns pulse) generating 12 guide stars of 25 Watts each, 8 Watt CW laser generating a single sodium guidestar, 12'th magnitude natural guide star, uncorrected.

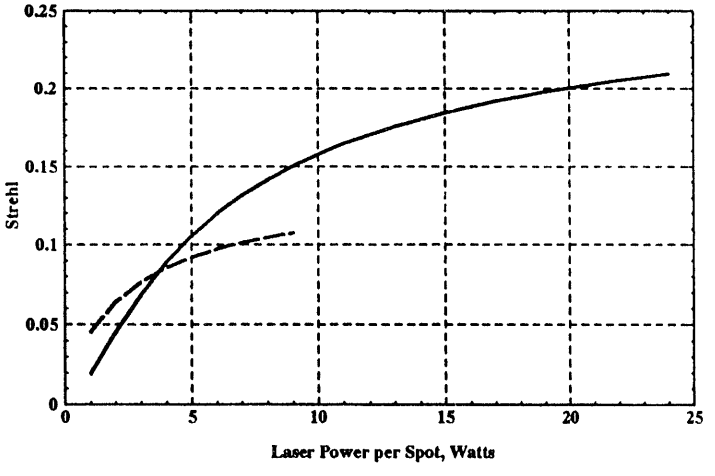

Figure 5 Strehl vs laser power at $\lambda = 0.7$ μm for a Keck 10 meter telescope adaptive optics system. 273 degree of freedom deformable mirror is assumed. Control bandwidth is optimized by trading servo lag error for signal photons at each point. Seeing conditions are $r_0 = 20$ cm, $f_g = 50$ Hz, $\theta_0 = 20$ μr at $\lambda = 0.5$ μm. Two cases are shown: solid curve is a pulsed dye laser (30 kHz, 150 ns pulse) generating 12 guide stars (each at the indicated power); dashed curve is a CW laser.

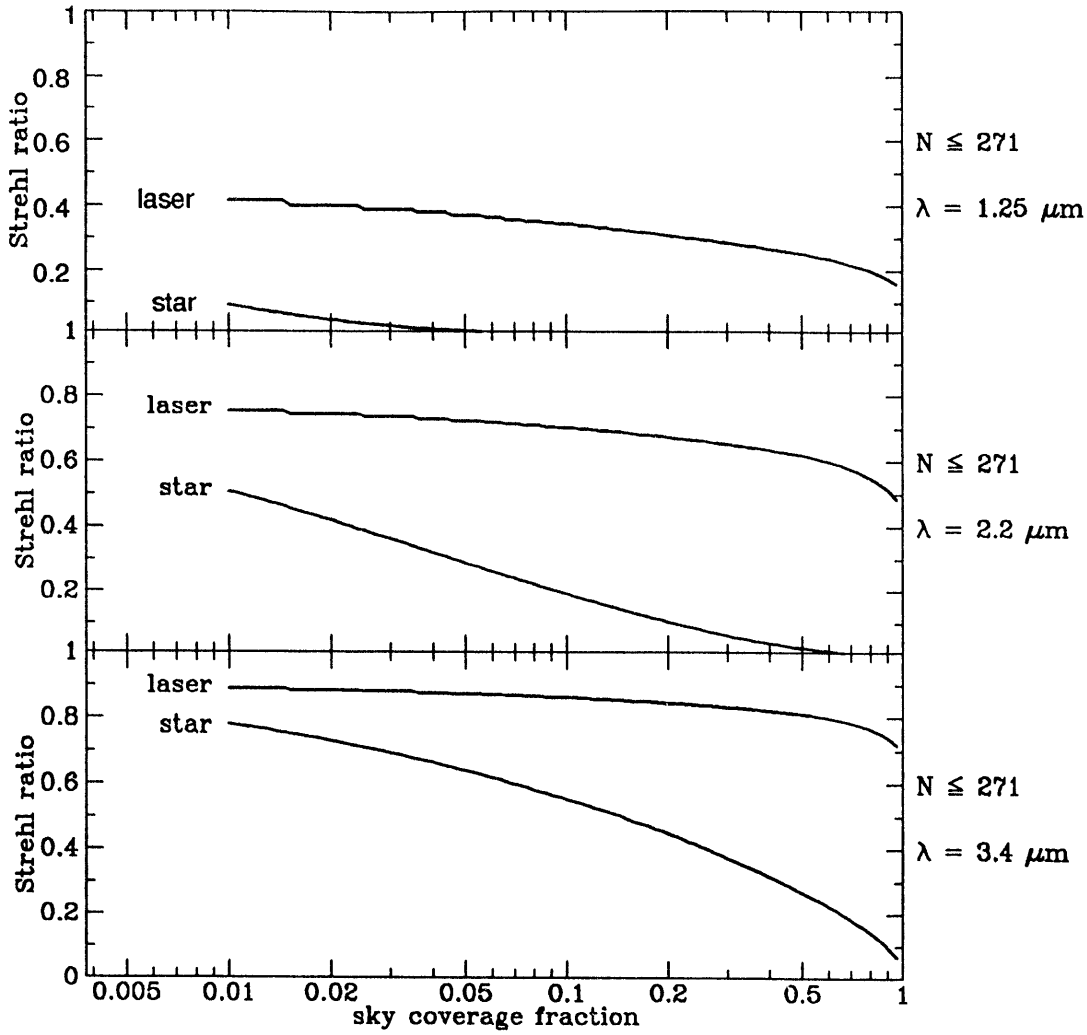

Figure 6 Sky coverage for laser and natural guide star adaptive optics systems. A 5 Watt CW laser is assumed. The natural wavefront reference star (tip/tilt reference star in the laser case) is chosen optimally, trading off separation angle for signal photons.

so much as a natural guide star system is degraded by wavefront anisoplanatism.

4. DISCUSSION

There remain several important issues that need to be addressed in the design of large telescope adaptive optics systems. For diffraction limited imaging in the visible, there needs to be developed a reliable and cost effective scheme for generating multiple laser guide stars, and for sensing the wavefronts individually. The obvious, but costly, approach is to simply duplicate the laser and wavefront sensor for each laser guide star. Certainly a clever scheme that is more suitable for observatory budgets would be of great benefit.

Wide field imaging is an important concern. Adaptive optics with its promised diffraction limited point spread function has the potential of revolutionizing high resolution spectroscopy. By reducing the slit width,

spectrometers can be designed to be physically smaller. But fiber fed spectrographs are inherently wide field instruments, and so far, adaptive optics systems appear to be limited to a small field of view a few isoplanatic angles across. Multi-conjugate adaptive optics systems (using several deformable mirrors) have been proposed to try to address this issue, but multi conjugate turbulence sensing will also be required. Again, a clever but low cost multi guide star scheme would benefit this application.

One final important issue is the cost of the wavefront reconstruction computer. The reconstruction algorithms that have been shown to work all require order n^2 calculations (where n is the number of degrees of freedom) at each wavefront reconstruction cycle, that is, at a rate typically ten times the closed loop bandwidth. The 69 actuator system at Lick Observatory accomplishes about 50 Hz bandwidth with four commercially available 50 gigaflop cpus running in parallel. Larger systems presently require special purpose parallel hardware. With thousands of degrees of freedom, the computer is by far the dominant cost item in the adaptive optics system, even more expensive than the laser. Clearly any breakthrough in wavefront reconstruction technique, say, that gives order $n \log n$ computational scaling, will greatly reduce the cost of a large adaptive optics system.

REFERENCES

1. J. M. Beckers, *Adaptive Optics for Astronomy: Principles, Performance and Applications*, **Annual Reviews of Astronomy and Astrophysics**, V. 31, 1993, also **ESO Scientific Preprint no.877**, October, 1992.
2. D. T. Gavel, J. R. Morris, and R. G. Vernon *Systematic Design and Analysis of Laser Guide Star Adaptive Optics Systems for Large Telescopes*, **J. Opt. Soc. Am.**, 11, 2, Feb. 1994, 914–924.
3. F. Chassat, *Theoretical Evaluation of the Isoplanatic Patch of an Adaptive Optics System Working Through the Atmospheric Turbulence*, **J. Optics (Paris)**, 20, 1, 1989, 12–23 (in French).
4. R. Sasiela, *A Unified Approach to Electromagnetic Wave Propagation in Turbulence and the Evaluation of Multiparameter Integrals*, **Lincoln Laboratory Technical Report No. 807**, July, 1988.
5. R. J. Noll, *Zernike Polynomials and Atmospheric Turbulence*, **J. Opt. Soc. Am.**, 66, 3, March, 1976, 207–211.
6. S. S. Olivier, *Performance of Adaptive Optics at Lick Observatory*, **SPIE 1994 Symposium on Astronomical Telescopes and Instrumentation for the 21'st Century** (This Conference), March 13–18, 1994.
7. M. Born and E. Wolf, **Principles of Optics**, Pergamon Press, Oxford, 1975, 463–460.
8. D. L. Fried, *Optical Resolution Through a Randomly Inhomogeneous Medium for Very Long and Very Short Exposures*, **J. Opt. Soc. Am.**, 56, 10, October, 1966, 1372–1379.
9. B. Welsh and C. Gardner, *Performance Analysis of Adaptive-optics Systems Using Laser Guide Stars and Slope Sensors*, **J. Opt. Soc. Am., A**, 6, 12, December, 1989 , 1913–1923.
10. H. W. Friedman, *Generation of a Sodium Guidestar Using a High Power Dye Laser*, **OSA Adaptive Optics for Large Telescopes Topical Meeting**, Technical Digest Series Volume 19, Lahaina, Maui, Hawaii, August 17–21, 1992, 210–212.
11. S. S. Olivier, C. E. Max, D. T. Gavel, and J. M. Brase, *Tip-Tilt Compensation: Resolution Limits for Ground Based Telescopes Using Laser Guide Star Adaptive Optics*, **Astrophysical Journal**, 407, April 10, 1993, 428–439.

END

DATE
FILMED
5/12/94